MULTIGRID METHODS FOR MONGE-AMPERE EQUATIONS

YE CHEN AND SCOTT R. FULTON*

Abstract. Best compact discretizations of a simple Monge-Ampere equation are found. It is verified that there is no fourth-order compact discretization of the Monge-Ampere equation. Multigrid methods combined with τ-extrapolation can solve the Monge-Ampere equation to fourth-order accuracy. A multigrid method is developed to solve the balanced vortex model (which involves a more complicated Monge-Ampere equation). This method works efficiently and is orders of magnitude faster than single-grid relaxations.

Key words. multigrid method, Monge-Ampere equation, balanced vortex model, compact discretization, conservative discretization, line relaxation, τ-extrapolation

AMS subject classifications. 65N55, 65N06, 65N22, 35J20, 35J60

1. Introduction. Monge-Ampere equations were first studied by G. Monge in 1784, and are receiving considerable interest because of their important role in several areas: differential geometry, Cauchy problems, etc. A Monge-Ampere equation (MAE) [7] is a second-order partial differential equation of the form $\psi_{xx}\psi_{yy} - \psi_{xy}^2 = a\psi_{xx} + 2b\psi_{xy} + c\psi_{yy} + \phi$, with coefficients depending on variables x, y, the unknown function ψ, and its first derivatives ψ_x, ψ_y.

The type of a MAE depends on the sign of the expression $\Delta = \phi + ac + b^2$. If $\Delta > 0$, it is of elliptic type; if $\Delta = 0$, it is of parabolic type; and if $\Delta < 0$, it is of hyperbolic type. In this paper, we will focus on elliptic MAEs only.

In section 2, by doing truncation analysis, the best compact discretizations of a simple MAE are obtained. Smoothing analysis has been done for each discretization with the Gauss-Seidel and Jacobi methods. Multigrid methods are used to test all the discretizations and relaxation schemes. Combining τ-extrapolation with multigrid can solve the MAE to fourth-order accuracy. A more complicated MAE (the balanced vortex model) is solved in section 3. Our conclusions are summarized in section 4.

2. Monge-Ampere equation. A simple elliptic MAE

$$(1 - \psi_{xx})(1 - \psi_{yy}) - \psi_{xy}^2 = f(x, y) \tag{2.1}$$

is considered on the unit square $\Omega = [0,1] \times [0,1]$ with Dirichlet boundary conditions, where $f(x,y) > 0$. Here we try to find a fourth-order 9-point compact discretization.

2.1. Compact discretizations. We consider discretizations of (2.1) on a uniform grid Ω^h of mesh size h of the form

$$L^h\psi = w^h f \tag{2.2}$$

where

$$L^h\psi = \Big(1 - A_y^h(a_1)D_{xx}^h\psi\Big)\Big(1 - D_{yy}^h A_x^h(a_1)\psi\Big) - \big(D_{xy}^h\psi\big)^2, \tag{2.3}$$

$$w^h f = c\Big(A_x^h(a_2) + A_y^h(a_2)\Big)f + S^h f. \tag{2.4}$$

Here, a_1, a_2 and c are constants, and the finite difference operators (D_{xx}^h, D_{yy}^h, and D_{xy}^h), the averaging operators ($A_x^h(a)$ and $A_y^h(a)$), and weighting oprator (S^h) are given (using stencil notation) by:

$$D_{xx}^h\psi = \frac{1}{h^2}\begin{bmatrix}1 & -2 & 1\end{bmatrix}\psi, \qquad A_x^h(a)\psi = \frac{1}{1+2a}\begin{bmatrix}a & 1 & a\end{bmatrix}\psi,$$

$$D_{yy}^h\psi = \frac{1}{h^2}\begin{bmatrix}1\\ -2\\ 1\end{bmatrix}\psi, \qquad A_y^h(a)\psi = \frac{1}{1+2a}\begin{bmatrix}a\\ 1\\ a\end{bmatrix}\psi,$$

$$D_{xy}^h\psi = \frac{1}{4h^2}\begin{bmatrix}-1 & 0 & 1\\ 0 & 0 & 0\\ 1 & 0 & -1\end{bmatrix}\psi, \qquad S^h = \begin{bmatrix}d & 0 & d\\ 0 & 0 & 0\\ d & 0 & d\end{bmatrix}.$$

*Department of Mathematics, Clarkson University, Campus Box 5815, Potsdam, NY 13699-5815 (chenye@clarkson.edu AND fulton@clarkson.edu).

Using the notation $\psi^{(m,n)} = \dfrac{\partial^{m+n}\psi}{\partial x^m \partial y^n}$ for partial derivatives of $\psi(x,y)$, and similarly for $f(x,y)$ in the Taylor expansion, and assuming $\psi(x,y) \in C^6$, one can obtain the truncation error of (2.2) in the form

$$\tau^h = w^h f - L^h \psi = Eh^2 + O(h^4), \tag{2.5}$$

where

$$\begin{aligned} E = \left(\frac{ca_2}{1+2a_2} + 2d\right) \Big[& -\psi^{(4,0)} - 2\psi^{(2,2)} - \psi^{(0,4)} + \psi^{(4,0)}\psi^{(0,2)} + 2\psi^{(3,0)}\psi^{(1,2)} + \psi^{(2,0)}\psi^{(2,2)} \\ & - 2\left(\psi^{(2,1)}\right)^2 - 2\psi^{(1,1)}\psi^{(3,1)} + \psi^{(0,4)}\psi^{(2,0)} + 2\psi^{(0,3)}\psi^{(2,1)} + \psi^{(0,2)}\psi^{(2,2)} - 2\left(\psi^{(1,2)}\right)^2 \\ & - 2\psi^{(1,1)}\psi^{(1,3)}\Big] + \frac{1}{12}\psi^{(4,0)} + \frac{2a_1}{1+2a_1}\psi^{(2,2)} + \frac{1}{12}\psi^{(0,4)} - \frac{1}{12}\psi^{(4,0)}\psi^{(0,2)} \\ & + \frac{a_1}{1+2a_1}\psi^{(2,2)}\left(\psi^{(0,2)} + \psi^{(2,0)}\right) + \frac{1}{12}\psi^{(0,4)}\psi^{(2,0)} - \frac{1}{3}\psi^{(1,1)}\left(\psi^{(1,3)} + \psi^{(3,1)}\right). \end{aligned} \tag{2.6}$$

To get a fourth-order compact discretization, one should choose the discretization parameters a_1, a_2, c and d properly so that $E = 0$. Unfortunately, from (2.6), E will not be zero since the terms $\psi^{(3,0)}\psi^{(1,2)}$, $(\psi^{(2,1)})^2$, $\psi^{(0,3)}\psi^{(2,1)}$ and $(\psi^{(1,2)})^2$, can not be eliminated. Thus, there is no fourth-order compact discretization to (2.1). We still can choose the parameters so that E is as small as possible if we know the properties of $\psi(x,y)$. Below we suppose $\psi(x,y)$ is unknown, and choose a_1, a_2, c and d to cancel as many terms in (2.6) as possible to obtain the best compact discretization to (2.1).

One approach is to set

$$\frac{ca_2}{1+2a_2} + 2d = \frac{1}{12} = \frac{a_1}{1+2a_1}, \tag{2.7}$$

so that some terms in (2.6) can be eliminated. Solving (2.7) yields $a_1 = \frac{1}{10}, a_2 = \frac{1-24d}{4+24d}, c = \frac{1}{2} - 2d$ with d a free parameter. The corresponding truncation error is

$$\begin{aligned} \tau_1 = \frac{h^2}{6}\Big[& \psi^{(3,0)}\psi^{(1,2)} - (\psi^{(2,1)})^2 + \psi^{(1,1)}\psi^{(1,3)} \\ & + \psi^{(1,1)}\psi^{(3,1)} - (\psi^{(1,2)})^2 + \psi^{(0,3)}\psi^{(2,1)}\Big] + O(h^4). \end{aligned} \tag{2.8}$$

With the natural choice $d = 0$ (which gives fewer operations), this discretization has $a_1 = \frac{1}{10}$, $a_2 = \frac{1}{4}$ and $c = \frac{1}{2}$. We refer to this as the MV discretization, since for the linearized problem (i.e., the Poisson equation) it is the "Mehrstellen Verfahren" discretization (which is fourth-order). Another approach is to set

$$\frac{ca_2}{1+2a_2} + 2d = \frac{1}{6} = \frac{a_1}{1+2a_1} \tag{2.9}$$

to cancel other terms in (2.6). Solving (2.9) yields $a_1 = \frac{1}{4}, a_2 = \frac{1-12d}{1+12d}, c = \frac{1}{2} - 2d$ with d free. The corresponding truncation error is

$$\begin{aligned} \tau_2 = \frac{h^2}{12}\Big[& -\psi^{(4,0)} - \psi^{(0,4)} + \psi^{(4,0)}\psi^{(0,2)} + \psi^{(0,4)}\psi^{(2,0)} \\ & + 4\left(\psi^{(3,0)}\psi^{(1,2)} + \psi^{(0,3)}\psi^{(2,1)} - (\psi^{(2,1)})^2 - (\psi^{(1,2)})^2\right)\Big] + O(h^4). \end{aligned} \tag{2.10}$$

Again, with $d = 0$, this reduces to $a_1 = \frac{1}{4}$, $a_2 = 1$, and $c = \frac{1}{2}$, which we refer to as the CY discretization.

Two special cases deserve mention. The discretization via standard central finite difference, which is commonly used, is the one corresponding to $a_1 = 0, a_2 = 0, c = \frac{1}{2}$ and $d = 0$. The truncation error then is

$$\begin{aligned} \tau_s = \frac{h^2}{12}\Big[& \psi^{(4,0)} + \psi^{(0,4)} - \psi^{(4,0)}\psi^{(0,2)} - \psi^{(0,4)}\psi^{(2,0)} \\ & + 4\left(\psi^{(1,1)}\psi^{(3,1)} + \psi^{(1,1)}\psi^{(1,3)}\right)\Big] + O(h^4). \end{aligned} \tag{2.11}$$

Also, if we set $a_1 = \frac{1}{2}, a_2 = 0, c = \frac{1}{2}$ and $d = 0$, we obtain a discretization of (2.1) with truncation error

$$\tau_c = \frac{h^2}{12}\Big[\psi^{(4,0)} + 6\psi^{(2,2)} + \psi^{(0,4)} - \psi^{(4,0)}\psi^{(0,2)} - \psi^{(0,4)}\psi^{(2,0)} \\ +4\psi^{(1,1)}\Big(\psi^{(3,1)} + \psi^{(1,3)}\Big) - 6\psi^{(2,2)}\Big(\psi^{(0,2)} + \psi^{(2,0)}\Big)\Big] + O(h^4) \tag{2.12}$$

We refer to this discretization as "conservative" since it approximately conserves area as in the coodinate transformation which underlies the MAE (2.1).

2.2. Relaxation scheme. The discrete equation (2.2) is a quadratic equation for $\psi_{i,j}$. Solving it yields the relaxation scheme

$$\psi_{i,j} \longleftarrow \frac{1}{2}\Bigg\{e_2 + e_3 - (1+2a_1)h^2 + \Bigg[\Big(e_2 + e_3 - (1+2a_1)h^2 - 4e_2e_3 + 4e_1(1+2a_1)h^2\Big)^2 \\ + (1+2a_1)^2h^4\Big([wf]_{i,j} - 1\Big) + \frac{1}{16}(1+2a_1)^2\psi^2_{\text{pmcorner}}\Bigg]^{\frac{1}{2}}\Bigg\}, \tag{2.13}$$

where the larger root is taken to preserve positive forcing. Here

$$e_1 = \frac{1}{4}\left[2a_1\psi_{\text{corner}} + (1-2a_1)\psi_{\text{udlr}}\right], \qquad e_2 = \frac{1}{2}\left[a_1\psi_{\text{corner}} - 2a_1\psi_{\text{ud}} + \psi_{\text{lr}}\right],$$
$$e_3 = \frac{1}{2}\left[a_1\psi_{\text{corner}} + \psi_{\text{ud}} - 2a_1\psi_{\text{lr}}\right], \qquad \psi_{\text{ud}} = \psi_{i,j+1} + \psi_{i,j-1},$$
$$\psi_{\text{corner}} = \psi_{i+1,j+1} + \psi_{i-1,j+1} + \psi_{i+1,j-1} + \psi_{i-1,j-1}, \qquad \psi_{\text{lr}} = \psi_{i+1,j} + \psi_{i-1,j},$$
$$\psi_{\text{pmcorner}} = \psi_{i+1,j+1} - \psi_{i-1,j+1} - \psi_{i+1,j-1} + \psi_{i-1,j-1}, \qquad \psi_{\text{udlr}} = \psi_{\text{ud}} + \psi_{\text{lr}},$$

and $[w^h f]_{i,j}$ is the value of $w^h f$ at grid point (i,j). This relaxation scheme is unweighted. If the value of $\psi_{i,j}$ is updated right after it is computed, it is the Gauss-Seidel method; if all values of $\psi_{i,j}$ are updated after a complete relaxation sweep, then it is the Jacobi method. We can also introduce a relaxation parameter ω to obtain the weighted relaxation scheme

$$\psi_{i,j} \longleftarrow (1-\omega)\,\psi_{i,j} + \omega\bar{\psi}_{i,j}, \tag{2.14}$$

where $\bar{\psi}_{i,j}$ is the value computed by the unweighted scheme (2.13).

2.3. Smoothing analysis. Smoothing analysis (also known as local Fourier analysis) is a powerful tool for designing an efficient multigrid method. Here we carry out one- and two-grid analysis (following the notation of [8]) on the linearization of the MAE (which is the Poisson equation) to predict the effectiveness of the smoothers discussed above.

2.3.1. One-grid analysis. After some calculation, one can find the symbol of the smoother for the Gauss-Seidel method (with lexicographic ordering) is

$$\tilde{S}_{\text{GS}}(\theta) = \frac{4(1-\omega) + \omega(1-2a_1)\left(\,e^{i\theta_1} + e^{i\theta_2}\,\right) + 4\omega a_1 e^{i\theta_2}\cos\theta_1}{4 - \omega(1-2a_1)\left(\,e^{-i\theta_1} + e^{-i\theta_2}\,\right) - 4\omega a_1 e^{-i\theta_2}\cos\theta_1}, \tag{2.15}$$

and the symbol for the Jacobi smoother is

$$\tilde{S}_{\text{Jac}}(\theta) = 1 - \omega + 2\omega a_1\cos\theta_1\cos\theta_2 + \frac{\omega}{2}(1-2a_1)\left(\cos\theta_1 + \cos\theta_1\right). \tag{2.16}$$

Here, $\theta = (\theta_1, \theta_2) \in [-\pi, \pi]^2$ is the discrete vector wavenumber. The smoothing factor is defined as the maximun absolute value of the symbol over the high modes $T^{\text{high}} := [-\pi,\pi)^2 \setminus \left[-\frac{\pi}{2}, \frac{\pi}{2}\right)^2$, i.e., $\mu_1 := \sup\left\{|\tilde{S}(\theta)| : \theta \in T^{\text{high}}\right\}$. Tables 2.1 and 2.2 list the smoothing factor of the Gauss-Seidel and Jacobi methods.

Table 2.1: Smoothing factor of the Gauss-Seidel method with lexicographic order

	μ_1		μ_2			
	$\omega = 1$	optimal	$\omega = 1$		optimal	
			V(1,1)	V(2,1)	V(1,1)	V(2,1)
$a_1 = 0$	0.5	0.5 ($\omega = 1.0$)	0.4387	0.4911	0.4387 ($\omega = 1.0$)	0.4874 ($\omega = 1.1$)
$a_1 = \frac{1}{10}$	0.4642	0.4642 ($\omega = 1.0$)	0.366	0.4209	0.366 ($\omega = 1.0$)	0.4169 ($\omega = 1.1$)
$a_1 = \frac{1}{4}$	0.4324	0.4323 ($\omega = 0.9$)	0.2709	0.4091	0.2653 ($\omega = 0.9$)	0.3904 ($\omega = 0.858$)
$a_1 = 0.5$	1.0	1.0 ($\omega = 1.0$)	0.99	1.0	0.99 ($\omega = 1.0$)	0.99 ($\omega = 1.0$)

Table 2.2: Smoothing factor of the Jacobi method with lexicographic order

	μ_1		μ_2			
	$\omega = 1$	optimal	$\omega = 1$		optimal	
			V(1,1)	V(2,1)	V(1,1)	V(2,1)
$a_1 = 0$	1.0	0.6 ($\omega = 0.8$)	1.0	1.0	0.6 ($\omega = 0.8$)	0.6 ($\omega = 0.8$)
$a_1 = \frac{1}{10}$	0.6	0.46 ($\omega = 0.9$)	0.6	0.6	0.46 ($\omega = 0.9$)	0.4687 ($\omega = 0.9$)
$a_1 = \frac{1}{4}$	0.5	0.3425 ($\omega = 0.895$)	0.5	0.5	0.3425 ($\omega = 0.895$)	0.4263 ($\omega = 0.9$)
$a_1 = 0.5$	1.0	1.0 ($\omega = 1.0$)	0.99	0.99	0.99 ($\omega = 1.0$)	0.99 ($\omega = 1.0$)

2.3.2. Two-grid analysis. The effects of grid transfers are included in two-grid analysis, so the two-grid smoothing analysis provides a more accurate prediction of the performance of a smoother. The effect of the two-grid cycle is measured by the asymptotic convergence factor

$$\rho(M_h^H) := \sup\left\{\rho\left(\hat{M}_h^H(\theta)\right) : \theta \in T^{\text{low}}, \theta \notin \Lambda\right\}. \tag{2.17}$$

Here, $\Lambda = \left\{\theta \in T^{\text{low}} : \tilde{L}_h(\theta) = 0 \quad \text{or} \quad \tilde{L}_H(\theta) = 0\right\}$, $\rho(\cdot)$ denotes the spectral radius, M_h^H is the two grid operator, $\hat{M}_h^H(\theta)$ is the representation of M_h^H on the harmonics space, $\tilde{L}_h$ is the symbol of the discrete operator, and h and H are the mesh size on fine and coarse grid, respectively.

For comparison with the one-grid smoothing analysis, it is convenient to calculate the corresponding two-grid smoothing factor, $\mu_2 = \sqrt[\nu]{\rho(M_h^H)}$, which estimates the convergence per fine-grid relaxation sweep. Here, $\nu = \nu_1 + \nu_2$ is the total number of sweeps performed per level in a multigrid V(ν_1, ν_2) cycle.

To compute the two-grid smoothing factor, we still need the symbol of the discrete operator L_h, the restriction operator I_h^H, and the prolongation operator I_H^h. The symbol of the discrete operator is

$$\tilde{L}_h(\theta) = \frac{-2}{(1+2a_1)h^2}\left[-2 + 4a_1\cos\theta_1\cos\theta_2 + (1-2a_1)(\cos\theta_1 + \cos\theta_2)\right]. \tag{2.18}$$

Full weighting will be used as the restriction operator, and the symbol is $\tilde{I}_h^H(\theta) = \frac{1}{4}(1+\cos\theta_1)(1+\cos\theta_2)$. For the prolongation operator, the natural choice is bilinear interpolation, whose symbol is $\tilde{I}_H^h(\theta) = \frac{1}{4}(1+\cos\theta_1)(1+\cos\theta_2)$. The two-grid smoothing factors are also listed in Table 2.1 and 2.2. By doing the smoothing analysis, especially the two-grid analysis, we learn that:

- The multigrid cycle V(1,1) has better smoothing factors than the V(2,1) cycle;
- For the Gauss-Seidel method, the unweighted version is optimal, and the weighted version ($\omega = 0.9$) of the Jacobi method is optimal.

- When $a_1 \geq 0.5$, the smoothing factors are greater than 0.9999 (i.e., the methods will not converge).

2.4. Numerical results. In this section, we will use all the discretizations and relaxation schemes described above to solve the nonlinear MAE (2.1) by multigrid methods. To test the solution methods, the analytical solution is specified as $\psi(x, y) = M_0 \dfrac{\cos[\lambda(1-y)]}{\cosh(\lambda x)}$, where $\lambda = 6.30505807$ and $M_0 = 0.02$. We use this function so that we can compare the numerical results obtained here with those for Boussinesq case in [1].

2.4.1. Test case. The four discretizations are considered: SD, CD, MV and CY. For $0.6 \leq \omega \leq 1.2$, we used both the Gauss-Seidel and Jacobi methods to solve (2.1). The numerical results show that the weighted version of Gauss-Seidel method does not give much improvement; and the Jacobi method is optimal when $\omega = 0.9$. From now on, nonGS denotes the unweighted version of Gauss-Seidel method, and 0.9WJ means the weighted version of Jacobi method with $\omega = 0.9$. Fig. 2.1–2.4 show the running time, numerical average convergence factor, truncation error and solution error for each discretization for different mesh sizes h. Fig. 2.1 shows the conservative discretization does not work for the MAE. The numerical convergence factors are larger than 1, and the solution errors are very large. From the numerical results, we can see that the Gauss-Seidel method works faster than the Jacobi method, and works for all the four discretizations. The Jacobi method will fail when the resolution is high.

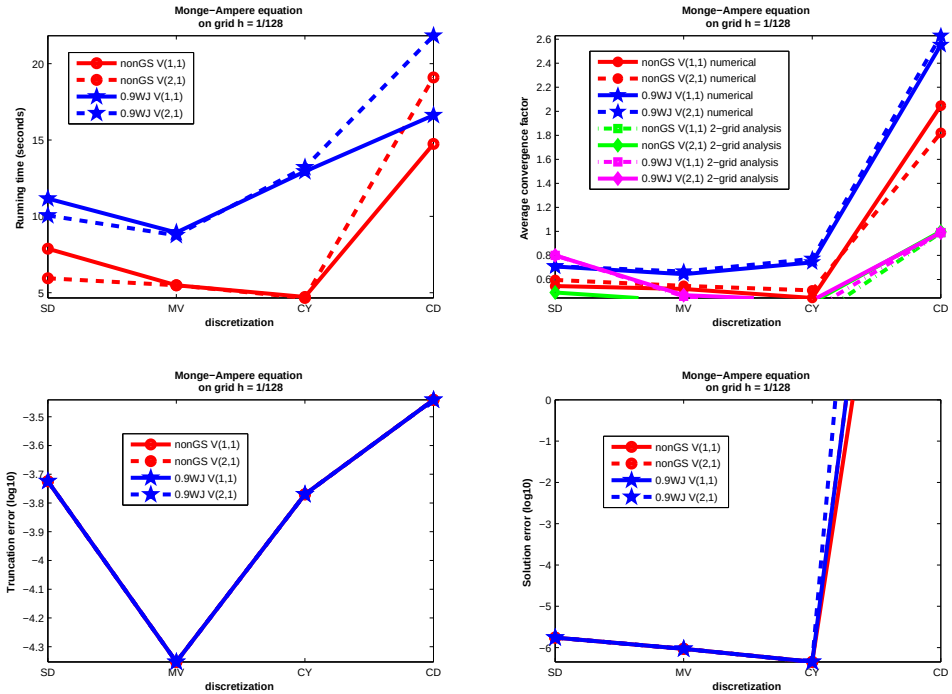

Fig. 2.1: MAE: conservative disretization does not work.

2.4.2. Double discretization. Both smoothing analysis and numerical experiments show that the conservative discretization will not work for the MAE. In an attempt to retain it for its conservation properties, we also considered double discretization, using the CD for residuals and another discretization (SD, MV or CY) for relaxation. Double discretizations can solve the problem, but they are not efficient (See Fig. 2.5, and compare with Fig. 2.2). They give large truncation errors and solution error, and converge slowly.

2.4.3. τ-extrapolation. To solve the MAE to fourth-order accuracy, a noncompact discretization can be used, e.g., $[\psi_{xx}]_{i,j} \approx (12h^2)^{-1} \begin{bmatrix} -1 & 16 & -30 & 16 & -1 \end{bmatrix} \psi + O(h^4)$. But this will involve more than

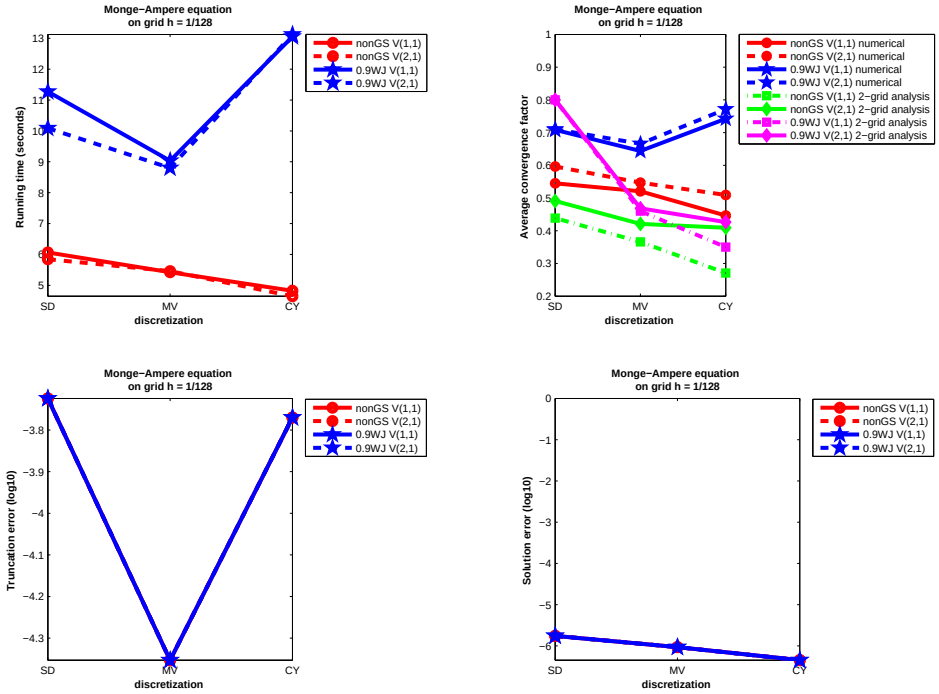

Fig. 2.2: MAE: nonGS vs. 0.9WJ, $h = 1/128$.

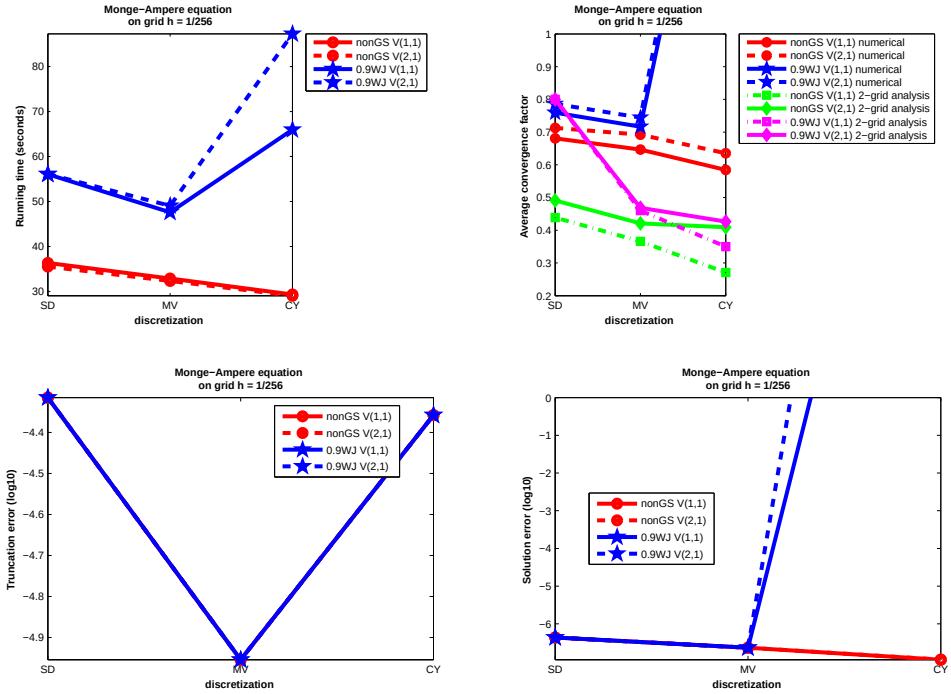

Fig. 2.3: MAE: nonGS vs. 0.9WJ, $h = 1/256$.

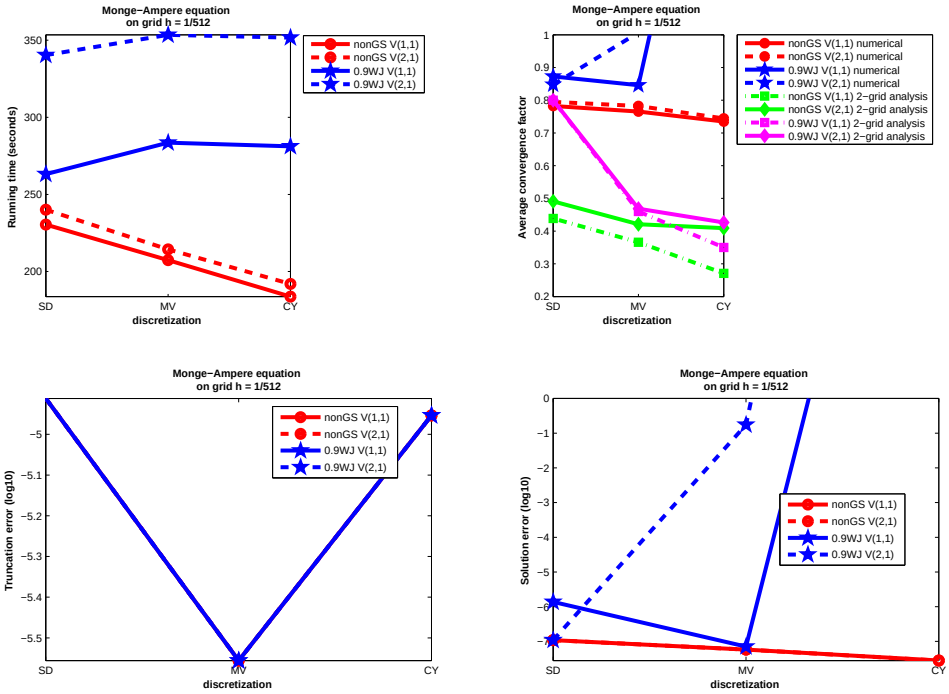

Fig. 2.4: MAE: nonGS vs. 0.9WJ, $h = 1/512$.

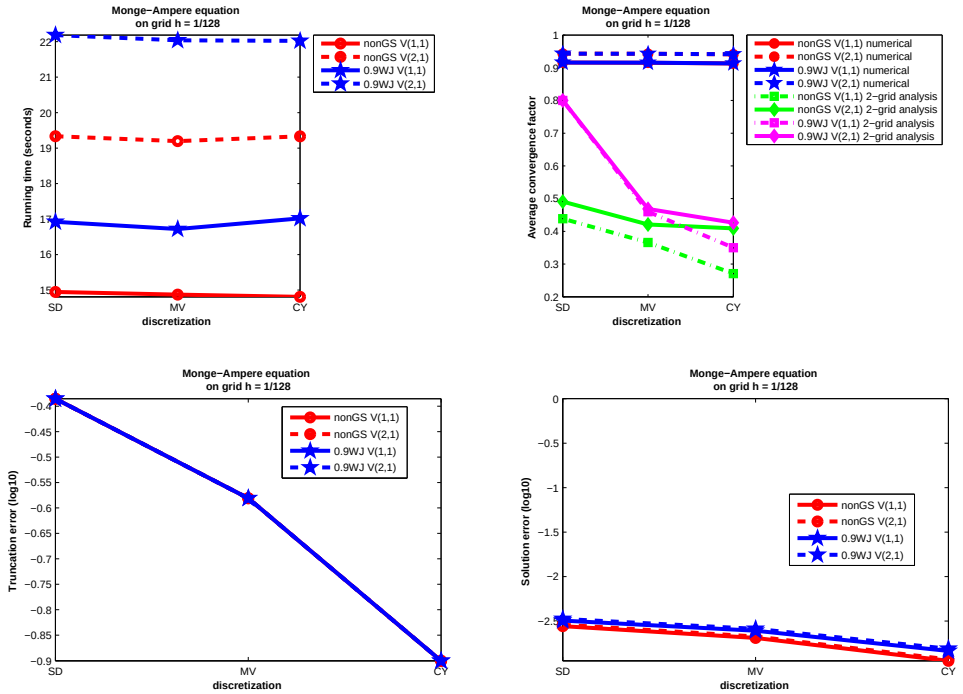

Fig. 2.5: MAE solved by doubl discretization; CD combined with SD, MV, or CY

9 points (maybe 25 points), and thus be more expensive. Also, formulating the discretization near the boundary will be difficult. Another approach is to combine the multigrid method with τ-extrapolation to yield higher-order accuracy. Various authors have studied τ-extrapolation (e.g., [4], [2] and [3]). We applied τ-extrapolation to the MAE, and the numerical results show that the problem can be solved to fourth-order accuracy. Figure 2.6 shows the MAE can be solved to fourth-order accuracy with τ-extrapolation even under a second-order discretization.

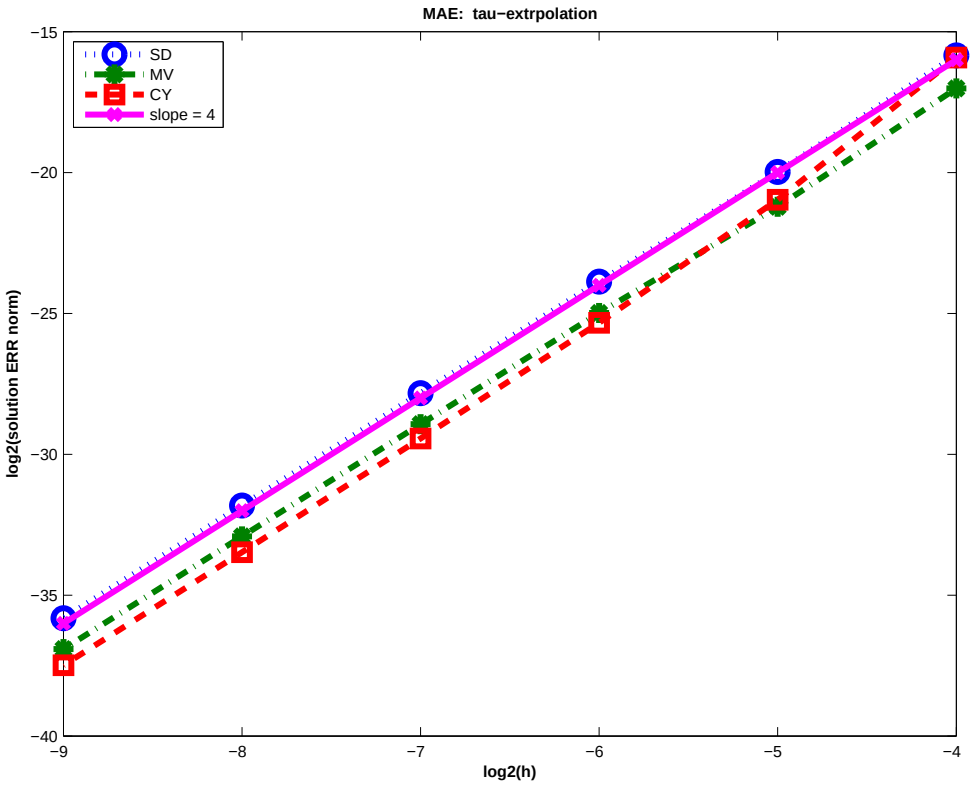

Fig. 2.6: MAE solved by τ-extrapolation under SD, MV, or CY discretizaion

3. Balanced vortex model. The balanced vortex model of Eliassen [5] describes circularly symmetric flows in gradient balance. Here we follow the formulation given by Schubert and Alworth [6]. It requires solving a nonlinear elliptic PDE of the Monge-Ampere type, refered to as the invertibility relation. This can be written as

$$\left[f^2 - R^3 \frac{\partial}{\partial R}\left(R^{-3}\frac{\partial M}{\partial R}\right)\right]\left[\frac{\partial^2 M}{\partial \Theta^2} - \bar{\Gamma}\sigma_0\right] + \left(\frac{\partial^2 M}{\partial R \partial \Theta}\right)^2 + \Gamma\sigma^*\left(f + \frac{2}{f}\frac{\partial M}{R\partial R}\right)^2 = 0, \tag{3.1}$$

with the boundary conditions

$$\frac{\partial M}{\partial \Theta} = 0, \qquad \text{at } \Theta = \Theta_T, \tag{3.2}$$

$$\left(f^2 + \frac{2}{R}\frac{\partial M}{\partial R}\right)\left(\Theta\frac{\partial M}{\partial \Theta} - M\right) + \frac{1}{2}\left(\frac{\partial M}{\partial R}\right)^2 = 0, \qquad \text{at } \Theta = \Theta_B, \tag{3.3}$$

$$\Gamma^{-1}\left(1 + \frac{2}{f^2}\frac{\partial^2 M}{\partial R^2}\right)^{-1}\left(\bar{\Gamma}\sigma_0 - \frac{\partial^2 M}{\partial \Theta^2}\right) = \sigma^*, \qquad \text{at } R = 0, \tag{3.4}$$

$$M = 0, \qquad \text{at } R = R_B. \tag{3.5}$$

Here, R (the potential radius) and Θ (the potential temperature) play the role of spatial coordinates, M is unknown (a Bernoulli function), σ^* is the forcing, f is the constant Coriolis parameter, σ_0 is a constant reference density, Γ depends on M via $\Gamma = \kappa\frac{\Pi}{p}$, $\Pi = \bar{\Pi} + \frac{\partial M}{\partial \Theta}$, $\bar{\Pi} = Cp\left(\frac{\bar{p}}{p_B}\right)^{\kappa}$, $-\frac{d\bar{p}}{d\Theta} = \bar{\sigma}$ ($\bar{\sigma}$ is a specified function of Θ), $p = p_B\left(\Pi/C_p\right)^{1/\kappa}$, $\bar{\Gamma} = \kappa\frac{\bar{\Pi}}{\bar{p}}$, $\kappa = 2/7$, $C_p = 287/\kappa$, and p_B and p_T are the pressure at the bottom and top boundaries, respectively. For more detail, see [6].

3.1. Discretization. We discretize the balanced vortex model on the grid defined by $R_i = i(\Delta R), i = 0, 1, 2, \cdots, n$; and $\Theta_j = \Theta_B + j\Delta\Theta, j = -1, 0, 1, 2, \cdots, m, m+1$. Here, we add ghost points in Θ-direction to handle the boundary conditions.

Expanding the term $R^3\frac{\partial}{\partial R}(R^{-3}\frac{\partial M}{\partial R}) = \frac{\partial^2 M}{\partial R^2} - \frac{3}{R}\frac{\partial M}{\partial R}$, and using central finite differences, the discrete form of the balanced vortex model is

$$\frac{f^2R_i^2\left(A_{i,j}B_{i,j} - C_{i,j}^2\right)}{\Gamma_{i,j}D_{i,j}^2(\Delta\Theta)^2} = \sigma_{i,j}^*, i = 1, 2, \cdots, n-1; j = 0, 1, \cdots, m. \tag{3.6}$$

Here

$$\begin{aligned}
A_{i,j} &= 2M_{i,j} - (\frac{3\Delta R}{2R_i} + 1)M_{i-1,j} + \left(\frac{3\Delta R}{2R_i} - 1\right)M_{i+1,j} + f^2(\Delta R)^2,\\
B_{i,j} &= 2M_{i,j} - M_{i,j+1} - M_{i,j-1} + \bar{\Gamma}_j\sigma_0(\Delta\Theta)^2,\\
C_{i,j} &= \frac{1}{4}(M_{i+1,j+1} - M_{i+1,j-1} - M_{i-1,j+1} + M_{i-1,j-1}),\\
D_{i,j} &= f^2R_i\Delta R + M_{i+1,j} - M_{i-1,j}.
\end{aligned}$$

The discrete forms of the boundary conditions are

$$\begin{aligned}
\frac{M_{i,j+1} - M_{i,j-1}}{2\Delta\Theta} &= 0, && j = m,\\
\left(f^2 + \frac{M_{i+1,j} - M_{i-1,j}}{R_i\Delta R}\right)\left(\Theta_B\frac{M_{i,j+1} - M_{i,j-1}}{2\Delta\Theta} - M_{i,j}\right) + \frac{1}{2}\left(\frac{M_{i+1,j} - M_{i-1,j}}{2\Delta R}\right)^2 &= 0, && j = 0,\\
B_{i,j}\Gamma_{i,j}^{-1}\left(1 + \frac{4}{f^2}\frac{M_{i+1,j} - M_{i,j}}{(\Delta R)^2}\right)^{-1} &= \sigma_{i,j}^*, && i = 0,\\
M_{n,j} &= 0, && i = n.
\end{aligned}$$

3.2. Relaxation scheme. The balanced vortex model is highly anisotropic, so point relaxation is not suitable. The strong coupling lies in the R-direction, so R-line relaxation will be applied. For each fixed j, the values $\mathbf{M}_j := [M_{1,j}, M_{2,j,}, \cdots, M_{n,j}]^T$, $(j = 0, 1, \cdots, m)$ are regarded as unknowns, and the values at adjacent R-lines ($j \pm 1$) are treated as knowns. The equations to be solved for $\mathbf{M}_j$ are

$$\mathbf{F}_{1,j}(\mathbf{M}_j) := f^2(\Delta R)^2B_{1,j} - \Gamma_{1,j}\sigma_{1,j}^*(\Delta\Theta)^2\left[\, f^2(\Delta R)^2 + 4M_{2,j} - 4M_{1,j}\,\right] = 0, \tag{3.7}$$

$$\mathbf{F}_{i,j}(\mathbf{M}_j) := f^2R_i^2\left(A_{i,j}B_{i,j} - C_{i,j}^2\right) - \Gamma_{i,j}\sigma_{i,j}^*(\Delta\Theta)^2D_{i,j}^2 = 0, \tag{3.8}$$

$$\mathbf{F}_{n,j}(\mathbf{M}_j) := M_{n,j} = 0. \tag{3.9}$$

One can write (3.7)-(3.9) in vector form as

$$\mathbf{F}_j(\mathbf{M}_j) = \mathbf{0}. \tag{3.10}$$

To solve (3.10), Newton's method is used, including two steps:

(1) Solve $-\frac{\partial\mathbf{F}_j}{\partial\mathbf{M}_j}(\Delta\mathbf{M}_j) = \mathbf{F}_j(\mathbf{M}_j)$;

(2) Update $\mathbf{M}_j \longleftarrow \mathbf{M}_j + \Delta\mathbf{M}_j$.

Here, $-\frac{\partial\mathbf{F}_j}{\partial\mathbf{M}_j}$ is the Jacobian matrix of the vector function $\mathbf{F}_j$. In this model, the system in step (1) is tridiagonal, so it can be solved efficiently. After doing relaxation on each R-line, the top and bottom boundary conditions are applied to set the vertical ghost points.

3.3. Numerical experiments. To compare with the results in [6], we use the same forcing, domain and resolution. The domain is $R_B = 1000$km, $\Theta_B = 300$K, and $\Theta_T = 360$K. The domain is divided into a 48×32 grid. The forcing is

$$\sigma^*(z,\tau) = \sigma_0 \begin{cases} e^{-\tau}, & z = 0, \\ \sin\Big(2\arctan\big(e^{-\tau}\tan\left(\frac{z}{2}\right)\big)\Big)\left(\sin z\right)^{-1}, & 0 < z < \pi, \\ e^{\tau}, & z = \pi, \end{cases} \tag{3.11}$$

where $\sigma_0 = (p_B - p_T)\,/\,(\Theta_T - \Theta_B)$, $p_B = 1000$mb, $p_T = 100$mb, $z = \pi\frac{\Theta - \Theta_B}{\Theta_T - \Theta_B}$, and $\tau = \pi\frac{\hat{Q}(R)T}{\Theta_T - \Theta_B}$. Here, $\hat{Q}(R) = Q_0 \exp\Big(-\left(R/R_0\right)^2\Big)$, and $R_0 = 250$km, $Q_0 = 30$K/day.

Point relaxation on single- and multi-grid are performed. On the single grid, the convergence is very slow, and it took 233735 seconds (64.93 hours) to obtain a solution. With a multigrid method, the point relaxation can work faster, 10800 seconds (3 hours) needed to get a solution. But when we solve the balanced vortex model using R-line relaxation with the multigrid method, only 48.96 seconds is needed.

4. Conclusion. Four discretizations of a simple MAE are discussed. MV gives the smallest truncation error, CY gives the smallest convergence factor and solution error, and CD does not work. Multigrid V(1,1) cycles work more efficient than V(2,1) cycles. The balanced vortex model is solved from time $T = 0$ hour to 96 hours. The performance degrades slightly when T is large (i.e. very forcing). In the future work, we will develop a robust multigrid method, based on the methods for (2.1), for the balanced vortex model and hopefully for general MAEs.

Acknowledgments. This work was funded in part by the National Science Foundation under grant No. ATM-0833057.

REFERENCES

[1] S. R. Fulton, *Multigrid solution of the semigeostrophic invertibility relation*, Mon. Wea. Rev., 117 (1989), pp. 2059–2066.
[2] S. R. Fulton, *On the accuracy of multigrid truncation error estimates*, ETNA, 15 (2003), pp. 29–37.
[3] A. Brandt, *Multigrid techniques: 1984 guide with application to fluid dynamics*, GMD, (1984).
[4] U. Rude, *Multiple τ-extrapolation for multigrid methods*, Tech. Rep. TUM-I8701, (1987).
[5] A. Eliassen, *Slow thermally or frictionally controlled meridional circulation in a circular vortex*, Astrophys. Norv., 5, 1952, pp. 19–60.
[6] W. H. Schubert and B. T. Alworth, *Evolution of potential vorticity in tropical cyclones*, Q. J. R. Meteorol. Soc., 113 (1987), pp. 147–162.
[7] R. Courant and D. Hilbert, *Methods of mathematical physics II*, Wiley, (1989), pp. 324.
[8] U. Trottenberg, C. W. Oosterlee, and A. Schuller, *Multigrid*, Academic Press, (2001).